IEEE Access
Multidisciplinary ⋮ Rapid Review ⋮ Open Access Journal

Received 30 January 2024, accepted 9 March 2024, date of publication 18 March 2024, date of current version 22 March 2024.

Digital Object Identifier 10.1109/ACCESS.2024.3378292

RESEARCH ARTICLE

An Efficient Joint Frame and Physical Layer Signaling Code Detection Method for DVB-S2

XIN-QI LIAO[1,2], (Member, IEEE), AND YIH-MIN CHEN[1,3]
[1]Department of Communication Engineering, National Central University, Taoyuan 30043, Taiwan
[2]National Chung-Shan Institute of Science and Technology, Taoyuan 32546, Taiwan
[3]Center for Astronautical Physics and Engineering, National Central University, Taoyuan 30043, Taiwan

Corresponding author: Xin-Qi Liao (111583001@cc.ncu.edu.tw)

ABSTRACT The Digital Video Broadcasting–Satellite Second Generation (DVB-S2) standard enhances coding and modulation techniques beyond those of DVB-S. It provides a spectrum of coding and modulation options (MODCOD) to suit diverse communication environments. Adaptive coding and modulation (ACM), along with additional signaling in the Physical Layer (PL) Header, are introduced, leading to potential ambiguities in frame synchronization and PL signaling identification for receivers. The straightforward approach is correlating the incoming DVB-S2 signal against all potential PL signaling codes. This process is computationally heavy and becomes impractical with all number of PL signaling codes. Addressing this challenge, this article presents an efficient approach utilizing the fast Walsh-Hadamard transform, significantly simplifying the frame detector's complexity. Furthermore, the detector facilitates MODCOD detection. The implementation of proposed architecture confirms the method in complexity reduction.

INDEX TERMS DVB-S2, frame synchronization, Fast Walsh Hadamard Transform, PLS code.

I. INTRODUCTION

The Digital Video Broadcasting – Satellite Second Generation (DVB-S2) is a standard in the realm of satellite broadband communication [1]. It was developed by the Digital Video Broadcasting (DVB) Project and officially released by the European Telecommunications Standards Institute (ETSI) in 2003. The DVB-S2 standard incorporates advanced LDPC (Low-Density Parity-Check) code and BCH (Bose–Chaudhuri–Hocquenghem) code, supplanting the Reed–Solomon (RS) code and convolutional code utilized in the DVB-S standard. These enhancements in coding techniques enable DVB-S2 to achieve lower bit error rates (BER) at reduced signal-to-noise ratios (SNR), thereby enhancing overall system performance. Moreover, DVB-S2 extends its modulation capabilities, including up to 32APSK modulation modes. This implies that, with appropriate code rates and SNR conditions, DVB-S2 can more efficiently utilize channel capacity, offering improved data transmission efficiency.

The associate editor coordinating the review of this manuscript and approving it for publication was Tianhua Xu.

The enhanced modulation schemes and coding rates in DVB-S2 afford a suite of flexible options tailored to various transmission scenarios. It brings out these options through adaptive coding and modulation (ACM) and variable coding and modulation (VCM) schemes, which are specified within the physical layer header. This adaptability ensures optimal performance across a spectrum of signal conditions.

The physical header of DVB-S2 dynamically adjusts its content in different transmission conditions, which poses a challenge for the receiver to synchronize the physical layer frame position and identify the signaling transmitted. Unlike the conventional DVB-S system, which relies on fixed frame structure, DVB-S2 with ACM/VCM makes frame synchronization and signaling identification less predictable.

The physical header of DVB-S2 consists of two key components: the Start of Frame (SOF) and the Physical Layer Signaling Code (PLSC). The SOF is a clear marker that indicates the start of each frame and segments the data stream into discrete units, while the PLSC conveys essential information for the receiver to demodulate the frame structure

correctly. This strategic integration enables the receivers to identify and process the incoming data frames efficiently, even with varying frame header lengths.

A review of state-of-the-art work indicates that frame synchronization can be divided into two approaches: coherent and noncoherent. Noncoherent approaches refer especially to frequency uncertainty due to Doppler from satellite motion. Differential correlation forms the maximum-likelihood approach, e.g., [2], [3], and [4], and post-detection integral base, e.g., [5], [6], and [7]. Another approach uses the modulation property of PL Header to synchronize frames, as in [8]. According to the specification [1], DVB-S2 should work even at as low as SNR -2.35dB. Adopting noncoherent approaches gains performance when frequency uncertainty exists but degrades performance in normal schemes. However, coherent approaches are in contrast. Therefore, there is a tradeoff between SNR performance and frequency uncertainty.

Additionally, to improve the signal-to-noise ratio, certain satellite communication systems operate with low-frequency offsets, such as Zhongxing 1E, Galaxy-34, SES-22, Measat 3D, etc. These satellites work in geostationary orbits but face challenges associated with low signal-to-noise ratios.

An intuitive approach for addressing frame synchronization is to create all modes of ACM/VCM correlation, which enables the determination of both the frame's location and the modulation and coding scheme employed. However, this method entails a significant consumption cost of resources in calculation.

This paper presents an efficient frame synchronization method for DVB-S2 system based on the fast Walsh-Hadamard transform. The proposed method reduces the computational complexity and improves the performance under extremely low signal-to-noise ratio. Also a maximum likelihood-based approach, as demonstrated by Massey gain improvement by simply adding a correction term. It is a simple way to implemnetation, therefore the Massey structure is adopted as the DVB-S2 synchronizer in this paper. The peak search algorithm is also optimized by exploiting the properties of the PLSC codes, which further enhances the frame synchronization and reduces the false alarm rate. The proposed method is implemented using FPGA and the resource usage and the synchronization time are evaluated, which demonstrate the feasibility and the efficiency of the method.

The rest of this paper is organized as follows. Section I introduces the Physical Layer frame structure and also gives model definitions to these utilities. Section II derives the PL Header and PLSC detection model and presents the proposed method. Section III focuses on implementing the method using FPGA and evaluating the resource usage and the synchronization time. Section IV compares the proposed method with other existing methods and analyzes the advantages and disadvantages. Section V concludes the paper with comprehensive reports.

FIGURE 1. DVB-S2 frame structure.

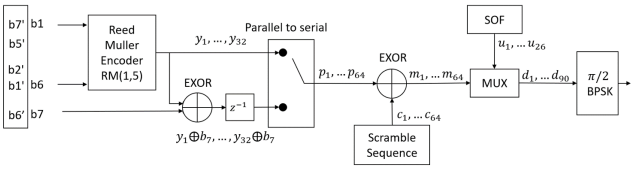

FIGURE 2. DVB-S2 transmitter block diagram.

II. TRANSMITTER FRAME STRUCTURE

The PL frame of DVB-S2 consists of PL Header and payload [1]. The DVB-S2 frame structure is shown in Figure 1.

The Start of Frame (SOF) is a 26-bit fixed unique word with 18D2E82(HEX) $\vec{u} = (u_1 \dots u_{26})$ which is attached in front of every frame. The PLSC costs 7 bits to represent 128 kinds of VCM/ACM signaling information which consist of MODCOD Field ($b_1\ b_2\ b_3\ b_4\ b_5$) and Type Field ($b_6\ b_7$) and remapping ($b_1\ b_2\ b_3\ b_4\ b_5\ b_6\ b_7$) into ($b'_7\ b'_5\ b'_4\ b'_3\ b'_2\ b'_1\ b'_6$). In the signaling information, the first 6 bits are computed with the following generator matrix G,where

$$G = \begin{pmatrix} 01010101010101010101010101010101 \\ 00110011001100110011001100110011 \\ 00001111000011110000111100001111 \\ 00000000111111110000000011111111 \\ 00000000000000001111111111111111 \\ 11111111111111111111111111111111 \end{pmatrix}$$

and each computation generate 32bits $\vec{y} = (y_1\ y_2 \dots y_{32})$. The generated sequence $\vec{y}$ replicates itself and performs exclusive or with the remaining signaling information bit b_7 after each output bit $\vec{p} = (y_1\, y_1 \oplus b_7\, y_2\, y_2 \oplus b_7 \dots y_{32}\ y_{32} \oplus b_7)$ denoted as $(p_1 p_2 \dots p_{64})$. The 64-bit serial sequence is scrambled with the code $\vec{c} = (c_1\ c_2 \dots c_{64})$ to obtain the PLSC $\vec{m} = (m_1\ m_2 \dots m_{64})$. Subsequently, the PLSC is integrated with the SOF to form a 90-bit PL Header, which is then modulated using pi/2-BPSK. The physical layer header transmitter system flow chart is depicted in Figure 2.

In their research, Feng-Wen Sun et al. argued that the Start of Frame (SOF) sequence is insufficiently long to provide the receiver with a high degree of confidence for successful frame detection [4]. The figure below shows the false detection rate depending on the pattern of SOF and the whole PL Header.

Thus, including the Physical Layer Signaling Code enhanced the probability of detection and emerged as a promising approach.

A. SIGNAL REPRESENTATION

Since the PL header $\vec{d} = (d_1 d_2 \dots d_{90})$ is mapped into pi/2 BPSK, regarding the binary data just control the phase of

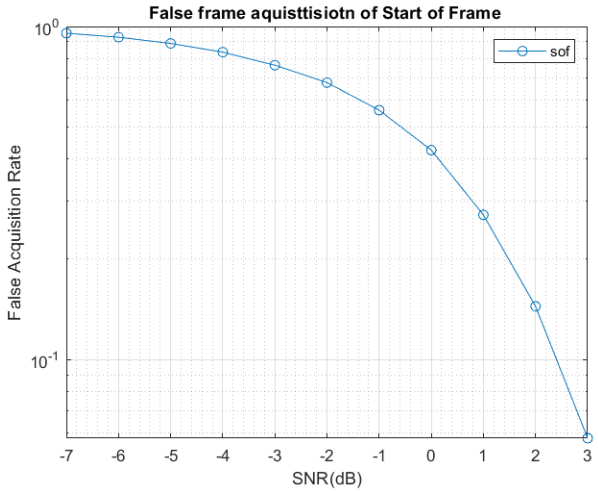

FIGURE 3. DVB-S2 frame false detection rate.

symbol is reasonable as (1) and (2). The SOF symbol signal can be represented as (1) with time index n.

$$s_n^{SOF} = e^{j(u_n\pi+\theta_n)} \tag{1}$$

The m^{th} PLSC signaling symbol signal can be represented as

$$s_n^{PLSC_m} = e^{j(m_n\pi+\theta_n)} \tag{2}$$

where θ_n is the phase of pi/2 BPSK, which is $(1+j)/\sqrt{2}$ for odd n and $(1-j)/\sqrt{2}$ for even n. (3) Separating the unscrambled PLSC sequence from the scrambled sequence results in two distinct signal terms, which can be defined as follows

$$s_n^{PLSC_m} = s_n^{p_m} \cdot s_n^c = e^{j(p_m\pi)} \cdot e^{j(c_n\pi+\theta_n)} \tag{3}$$

$s_n^{p_m}$ controls the sign of s_n^c. Listing $s_n^{p_m}$ by m from 0 to 127 and permuting in array $S_P^T = \left[s_n^{p_0\,T}\ s_n^{p_1\,T}\ \ldots\ s_n^{p_{127}\,T}\right]$. $(*)^T$ denote transport computation. Corresponding 1 to black and 0 to white in the array and displaying as an image shown in Figure 4.

Observation reveals that the difference between even and odd rows is determined by the signum function. To reconstruct the array S_P, even and odd rows are separated, denoted as W and $-W$ respectively, and shown as such in Figure 5(a) for even rows and Figure 5(b) for odd rows.

The matrix is Hadamard matrix in dyadic order and the rows of W is a Walsh function set [9]. Representation the element of y^{th} row x^{th} column is

$$w_x^y = (-1)^{\sum_{b=1}^{6} y_{b-1}x_{6-b}} \tag{4}$$

where x_b and y_b in (4) are binary bit of time index x and othogonal serial stamp y which shown in

$$x = \sum_{b=1}^{6} 2^{x_b},\ x = 0, \ldots, 63 \tag{5}$$

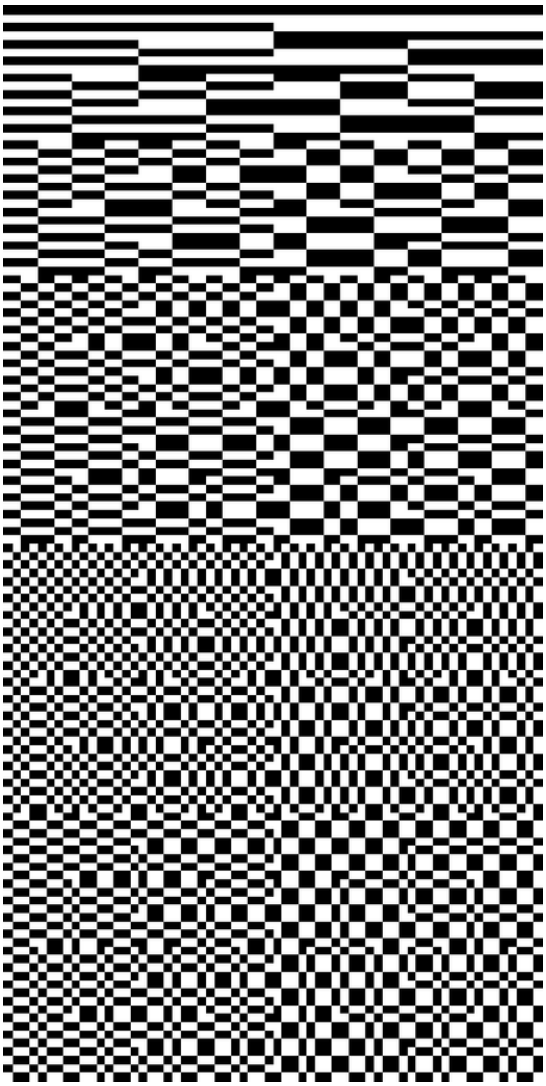

FIGURE 4. Array of encoded matrix in gray scale.

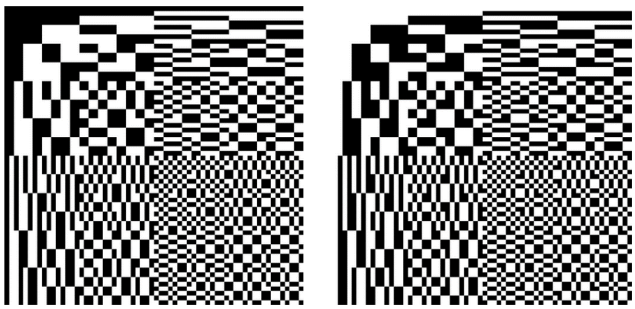

FIGURE 5. Even row extraction (a); Odd row extraction (b).

$$y = \sum_{b=1}^{6} 2^{y_b}\ y = 0, \ldots, 63 \tag{6}$$

Hence,the unscramble sequence of PLSC $s_n^{p_m}$ can express as following equation

$$s_n^{p_m} = a_m \cdot w_n^{\lfloor \frac{m}{2} \rfloor} \tag{7}$$

where $\lfloor * \rfloor$ represents the floor function, and m denotes the signaling mode, ranging from 0 to 127. The scalar a_m is equal to 1 when the signaling mode is even and -1 when the signaling mode is odd. Finally, the PL frame can express as

$$s_n^{PLF_m} = \begin{cases} s_n^{PLH_m}, & n = 1, \ldots, 90 \\ s_{n-90}^{payload_m}, & n = 91, \ldots, NF_m \end{cases} \tag{8}$$

where $s_n^{payload_m}$ denote payload symbol which decided by the PLSC symbol $s_n^{PLSC_m}$ when m^{th} signaling is transmitting. And the PL Header can express as

$$s_n^{PLH_m} = \begin{cases} s_n^{SOF}, & n = 1, \ldots, 26 \\ s_{n-26}^{PLSC_m} & n = 27, \ldots, 90 \end{cases} \tag{9}$$

III. RECEIVED SIGNALING DETECTION

Assuming perfect synchronization with symbol timing and phase when receiving incoming frame $s_n^{PLF_m}$ with m^{th} signaling transmitting over an AWGN channel.

$$r_n = s_n^{PLF_m} + g_n \tag{10}$$

where g_n is complex AWGN noise with power spectrum density N_0 First, assuming precise frame synchronization at index k, the subsequent task involves the identification of the Physical Layer signaling code index denoted as m from the header. This process is characterized by the conditional probability density function of vector $\vec{r} = (r_1\ r_2 \ldots r_{PLF})$, represented in the equation below:

$$f\left(\vec{r}\middle|m,k,\vec{d}\right) = \prod_{n=1}^{N_{PLH}} \left(\frac{1}{\pi N_0}\right) \cdot e^{-\frac{\left(r_{n+k} - s_{n+k}^{PLF_m}\right)^2}{N_0}} \tag{11a}$$

$$= \left(\frac{1}{\pi N_0}\right)^{N_{PLF}} \cdot \prod_{n=1}^{N_{PLH}} e^{-\frac{\left(r_{n+k} - s_{n+k}^{PLF_m}\right)^2}{N_0}} \cdot \prod_{n=N+1}^{N_{PLF}} e^{-\frac{\left(r_{n+k} - s_{n+k}^{Payload}\right)^2}{N_0}} \tag{11b}$$

Assume frame length is N_{PLH} where can divide into PL Header part with length N_{PLH} and Payload part $N_{PLF} - N_{PLH}$.

A. SIGNALING DETECTION

Taking natural logarithm to likelihood function in (11b), a joint optimum decision of frame index $\hat{m}$ and PLSC $\hat{k}$ is:

$$\left(\hat{m},\hat{k}\right) = \arg\max_{m,k} \ln\left(f\left(\vec{r}\middle|m,k,\vec{d}\right)\right) \tag{12a}$$

$$= \arg\max_{m,k} \left(\sum_{n=1}^{N_{PLH}} r_{n+k} \cdot s_{n+k}^{PLF_m} + \sum_{n=N_{PLH}+1}^{N_{PLF}} r_{n+k} \cdot s_{n+k}^{Payload} \right) \tag{12b}$$

Assume PSK payload have been sufficiently scrambled to have equal probability property so the expectation nearly

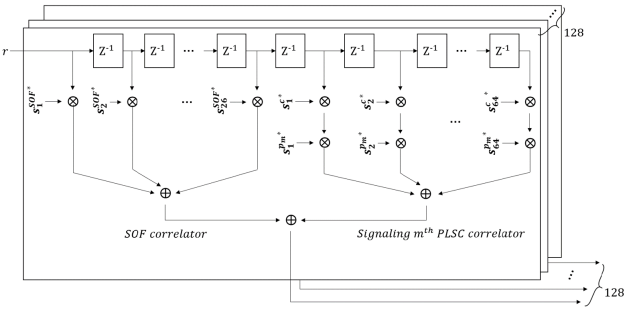

FIGURE 6. Frame and PLSC detection block diagram.

$(1/M)^{N_{PLF}-N+1} \sum_{\vec{d}} a_k e^{j\theta_k}$ to zero [3]. The optimum decision for PLSC m and frame index k of (12b) should be like:

$$\left(\hat{m},\hat{k}\right) = \arg\max_{m,k} \left(\sum_{n=1}^{N_{PLH}} r_{n+k} \cdot s_{n+k}^{PLF_m} \right) \tag{13}$$

Separating the start of frame signal from the $s_{n+k}^{PLF_m}$, the likelihood function in (13) of physical layer signaling detection can be rewritten as follows:

$$\left(\hat{m},\hat{k}\right) = \arg\max_{m,k} \left(\sum_{n=1}^{N_{SOF}} r_{n+k} \cdot s_{n+k}^{SOF} + \sum_{n=N_{SOF}+1}^{N_{PLH}} r_{n+k} s_{n+k}^{PLSC_m} \right) \tag{14}$$

Taking into account the fixed nature of the SOF pattern, it is feasible to execute the PLSC decision apart from (14), denoted as m before the completion of frame synchronization. This concept can be expressed mathematically as follows:

$$\left(\hat{m},\hat{k}\right) = \arg\max_{k} \left(\sum_{n=1}^{N_{SOF}} r_{n+k} \cdot s_{n+k}^{SOF} + \arg\max_{m} \left\{ \sum_{n=N_{SOF}+1}^{N_{PLH}} r_{n+k} \cdot s_{n+k}^{PLSC_m} \right\} \right) \tag{15}$$

The block diagram of the frame and PLSC detection is shown in Figure 6 under the conditional PLSC known assumption. In order to make the detection system more efficient, trimming the term of the equation by using the biorthogonal property of the PLSC sequence. Recall the former description, all possible signaling signals $s_n^{PLSC_m}$ form a biorthogonal signal set with the following correlation property:

$$\sum_{n=1}^{N} s_n^{PLSC_i} \left(s_n^{PLSC_j}\right)^* = \begin{cases} N, & i = j \\ -N, & i = j+1 \\ 0, & \text{otherwise} \end{cases} \tag{16}$$

where N represents the length of the scramble sequence, which is fixed at 64. It is important to observe that the cross-correlation between adjacent PLSC indices exhibits a distinctive characteristic compared to autocorrelation, primarily in terms of its sign. The approach of trimming

the adjacent PLSC correlation for the decision rule can be represented as follows:

$$\left(\hat{j},\hat{k}\right) = \arg\max_{k}\Big(\sum_{n=1}^{N_{SOF}} r_{n+k}\cdot s_{n+k}^{SOF} + \arg\max_{j}\left\{\Big|\sum_{n=N_{SOF}+1}^{N_{PLH}} r_{n+k}\cdot s_{n+k}^{PLSC_m}\Big|\right\} \quad (17)$$

Furthermore, the process of (17) determining the sign decision is achieved through the representation of the index remainder i as following

$$i = \begin{cases} 0, & \sum_{n=N_{SOF}+1}^{N_{PLH}} r_{n+k}\cdot s_{n+k}^{PLSC_{\hat{j}}} \geq 0 \\ 1, & \sum_{n=N_{SOF}+1}^{N_{PLH}} r_{n+k}\cdot s_{n+k}^{PLSC_{\hat{j}}} < 0 \end{cases} \quad (18)$$

where $\hat{m} = \hat{j} + i$ computation in two parts above.

1) EFFICIENCY DESIGN FOR PLSC

As a consequence of the composition of $s_n^{PLSC_m}$, as described in Section II-A along with the pi/2 BPSK symbol mapping and the scramble operation, which primarily involves a phase adjustment applied to s^{PLSC_m}, we can define the corrected frame synchronization received PLSC as r_n^{PLSC}. The correlation component can then be expressed as follows

$$c_m = \sum_{n=1}^{N} r_n^{PLSC}\cdot s_n^{PLSC_m\,*} = a^m \cdot \sum_{n=1}^{N} r_n^{PLSC}\cdot s_n^{c*}\cdot w_n^{\lfloor \frac{m}{2} \rfloor} \quad (19)$$

It is noteworthy that the correlation term can be expressed as a linear combination utilizing Walsh functions, which can be equivalently interpreted as a form of the Fast Walsh-Hadamard Transform [10]. Consequently, the decision rule (18) can be redefined as follows.

$$\left(\hat{j},\hat{k}\right) = \arg\max_{k}\Big(\sum_{n=1}^{N_{SOF}} r_{n+k}\cdot s_{n+k}^{SOF} + \arg\max_{j}\left\{\left|FWHT_N\left\{r_{n+\hat{k}}^{PLSC}\cdot s_n^{c*}\right\}\right|\right\} \quad (20)$$

After $\hat{k}$ is discovery, the remainder index i decision rule (18) becomes (21) with property form (19)

$$i = \begin{cases} 0, & FWHT_N\left\{r_{n+\hat{k}}^{PLSC}\cdot s_n^{c*}\right\} \geq 0 \\ 1, & FWHT_N\left\{r_{n+k}^{PLSC}\cdot s_n^{c*}\right\} < 0 \end{cases} \quad (21)$$

PLSC MODCOD and Type field can be reconigze after behind. The figure below provides a schematic diagram of the continuous transmission of multiple frames, with PLSC indices [32 32 33 33 32 32 44 44 32 32] in sequence. Each received signal is unfolded in three-dimensional space after FWHT operation. From the figure8, it can be observed that the correct PLSC index and Time index of the maximum value occur.

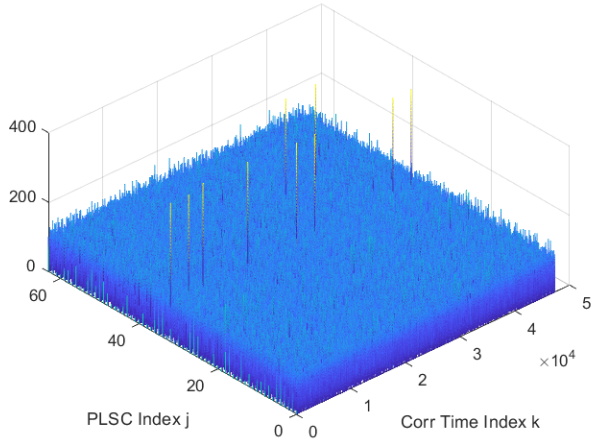

FIGURE 7. Demonstration of detector.

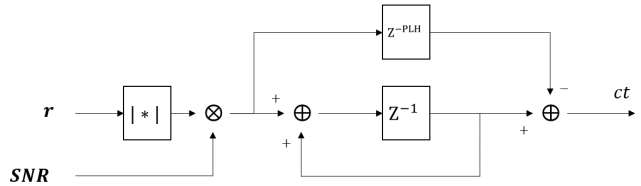

FIGURE 8. Correction term block diagram.

2) CORRECTION TERM OF DETECTION

Massey derived the Maximum Likelihood method by adding a correction term in the correlator [11], which is given in the following equation:

$$ct = SNR \cdot \sum_{l=1}^{N_{PLH}} |r_{n+l}| \quad (22)$$

And its corresponding block diagram is shown in Figure 8.

The magnitude computation is frequently implemented in approximate models or approached using the CORDIC algorithm. This paper adopts an approximation model by [12] and [13], which is given in the following equation

$$magnitude \approx \max(|I|,|Q|) + 0.5\cdot\min(|I|,|Q|) \quad (23)$$

In this approximation model, the root mean square (rms) deviation is -20.7 dB, while the peak deviation is -18.6 dB.

3) PERFORMANCE

The figure shows the simulation comparing executing frame synchronization by only the frame start indicator, the entire physical layer header, and the entire physical layer header with the correction term. From Figure 9, the performance of False Detected Rate does improve after adding correction terms to the detector in (20).

IV. IMPLEMENTATION

From a hardware implementation perspective, the utilization of the Fast Walsh-Hadamard Transform within the PLSC detector is pivotal. It offers an efficient approach to resource

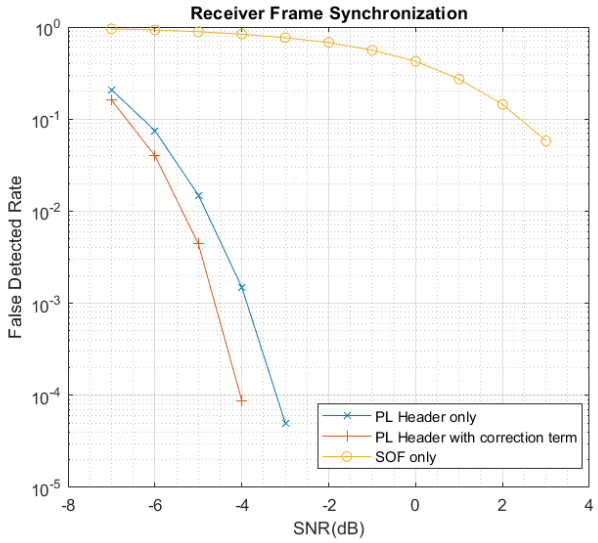

FIGURE 9. False acquisition rate of different frame synchronization methods.

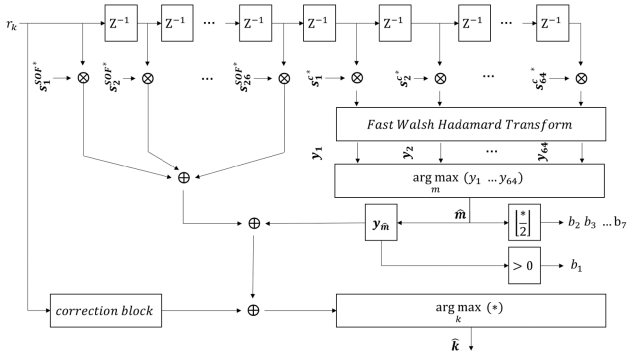

FIGURE 10. Efficient frame and PLSC detection block diagram.

sharing by facilitating the demapping and descrambling of received symbols. The initial detection design necessitated the deployment of 128 sets of detectors to accommodate all physical layer signaling modes. However, through the implementation of the Fast Walsh-Hadamard Transform as discussed in Section III.B, a substantial reduction in register usage can be achieved. To illustrate the proposed scheme, a block diagram combining the frame and physical layer signaling detector is presented in Figure 10.

1) FPGA DESIGN UTILIZATION

The proposed method has been implemented on the Xilinx FPGA device xc7z020clg484-1 successfully. Concurrently, this paper also presents the implementation of the physical layer signaling detector without the efficiency-oriented design with PSLC partial Mode while only obtaining 32 groups due to being limited by the gate count number of FPGA. In the implementation of the Xilinx device xczu9egffvb1156-2 which carries much more gate count than xc7z020clg484-1, a detailed comparison of resource

TABLE 1. Hardware utilization comparison.

	Propose Design	Inefficiently Design (Partial Mode)
Device	xc7z020clg484-1	xczu9egffvb1156-2
Slice LUTs	9686	202414
Slice Registers	11027	10338
DSP48E	NA	NA
Speed	200MHz	100MHz

utilization between the two designs is provided in the table below. As the result, generalizing the results of 32 groups to 128 groups, the LUT utilization should require at least 80k, and the register utilization should require at least 40k. Compared to the efficient design, the inefficient design requires approximately 80 times more LUT usage and about 4 times more register usage.

V. CONCLUSION

The DVB-S2 standard, an advancement over DVB-S, offers enhanced coding and modulation techniques, providing a range of suitable options for various scenarios. However, it also introduces dynamic changes to the Physical Layer Header, complicating the design of receivers. This article proposes reordering the MODCOD and Type Field bits to present the PLSC sequence in Dyadic order, as generated by the Walsh function. Hence, receivers can significantly reduce the resources needed for frame synchronization and jointly detect the PLSC using the Fast Walsh-Hadamard Transform. In terms of hardware implementation, this paper demonstrates the intuitive approach with the xczu9egffvb1156-2 platform and implements the proposed architecture on the xc7z020clg484-1 platform. The proposed architecture of joint PLSC and frame deterctor greatly lowing the LUT around 80 times and register around 4 times via Fast Walsh-Hadamard Transform.

REFERENCES

[1] *Digital Video Broadcasting (DVB); Second Generation Framing Structure, Channel Coding and Modulation Systems for Broadcasting, Interactive Services, News Gathering and Other Broadband Satellite Applications*, Digital Video Broadcasting (DVB), Geneva, Switzerland, 2005.

[2] Z. Y. Choi and Y. H. Lee, "On the use of double correlation for frame synchronization in the presence of frequency offset," in *Proc. IEEE Int. Conf. Commun.*, Jun. 1999, pp. 958–962.

[3] Z. Yong Choi and Y. H. Lee, "Frame synchronization in the presence of frequency offset," *IEEE Trans. Commun.*, vol. 50, no. 7, pp. 1062–1065, Jul. 2002.

[4] F. Sun, Y. Jiang, and L. Lee, "Frame synchronization and pilot structure for second generation DVB via satellites," *Int. J. Satell. Commun. Netw.*, vol. 22, no. 3, pp. 319–339, May 2004.

[5] P. Kim, G. E. Corazza, R. Pedone, M. Villanti, D.-I. Chang, and D.-G. Oh, "Enhanced frame synchronization for DVB-S2 system under a large of frequency offset," in *Proc. IEEE Wireless Commun. Netw. Conf.*, Mar. 2007, pp. 1183–1187.

[6] G. E. Corazza and R. Pedone, "Maximum likelihood post detection integration methods for spread spectrum systems," in *Proc. IEEE Wireless Commun. Netw. (WCNC)*, Mar. 2003, pp. 227–232.

[7] A. J. Viterbi, *CDMA: Principles of Spread Spectrum Communication*, 1st ed. Reading, MA, USA: Addison-Wesley, 1995.

[8] H. Wu, H. Xie, Z. T. Huang, and Y. Y. Zhou, "Frame synchronization for DVB-S2 in physical layer header code uncertainty," *Appl. Mech. Mater.*, vols. 543–547, pp. 2632–2635, Mar. 2014.

[9] C. Geadah, "Natural, dyadic, and sequency order algorithms and processors for the Walsh-Hadamard transform," *IEEE Trans. Comput.*, vol. C-26, no. 5, pp. 435–442, May 1977.
[10] A. Fino, "Unified matrix treatment of the fast Walsh–Hadamard transform," *IEEE Trans. Comput.*, vol. C-25, no. 11, pp. 1142–1146, Nov. 1976.
[11] J. Massey, "Optimum frame synchronization," *IEEE Trans. Commun.*, vol. COM-20, no. 2, pp. 115–119, Apr. 1972.
[12] R. Lyons, *Understanding Digital Signal Processing*, 3rd ed. London, U.K.: Pearson, 2010.
[13] M. C. Jeruchim, P. Balaban, and K. S. Shanmugan, *Simulation of Communication Systems: Modeling, Methodology and Techniques (Information Technology: Transmission, Processing and Storage)*, 2nd ed. Cham, Switzerland: Springer, 2000.

XIN-QI LIAO (Member, IEEE) received the Bachelor of Science degree in electrical engineering from the National Taipei University of Technology, the Master of Science degree in communication engineering from National Central University in 2016, where he is currently pursuing the Ph.D. degree in communication engineering. He has employed at the Information and Communication Division, National Chung-Shan Institute of Science and Technology, Taoyuan, Taiwan.

YIH-MIN CHEN received the B.S., M.S., and Ph.D. degrees in electrical engineering from National Taiwan University, Taipei, Taiwan, in 1982, 1986, and 1991, respectively. From 1990 to 2001, he was an Associate Professor with the Department of Electrical Engineering, Yuan Ze University. From 1998 to 1999, he was temporarily on leave from Yuan Ze University and served as a Visiting Scientist with the Research Laboratory of Electronics, Massachusetts Institute of Technology, with a scholarship awarded by the National Science Council. From 2001 to 2003, he was with the Department of Communication Engineering, Yuan Ze University. Since 2021, he has been with the Center for Astronautical Physics and Engineering, National Central University. He is currently an Associate Professor with the Department of Communication Engineering, National Central University, Taiwan. His current research interests include software-defined radio architecture design and implementation, baseband signal processing for wireless communications, embedded software for digital signal processors, and signal processing for multiple antennas.